

# A combined environmental scanning electron microscopy and Raman microscopy study of methanol oxidation on silver(I) oxide

Graeme J. Millar\*, Megan L. Nelson and Phillipa J.R. Uwins<sup>a</sup>

*Department of Chemistry and Centre for Microscopy and Microanalysis<sup>a</sup>, The University of Queensland, St. Lucia, Brisbane, Queensland 4072, Australia*

Received 12 February 1996; accepted 10 May 1996

The techniques of environmental scanning electron microscopy (ESEM) and Raman microscopy have been used to respectively elucidate the morphological changes and nature of the adsorbed species on silver(I) oxide powder, during methanol oxidation conditions. Heating  $\text{Ag}_2\text{O}$  in either water vapour or oxygen resulted firstly in the decomposition of silver(I) oxide to polycrystalline silver at 578 K followed by sintering of the particles at higher temperature. Raman spectroscopy revealed the presence of subsurface oxygen and hydroxyl species in addition to surface hydroxyl groups after interaction with water vapour. Similar species were identified following exposure to oxygen in an ambient atmosphere. This behaviour indicated that the polycrystalline silver formed from  $\text{Ag}_2\text{O}$  decomposition was substantially more reactive than silver produced by electrochemical methods. The interaction of water at elevated temperatures subsequent to heating silver(I) oxide in oxygen resulted in a significantly enhanced concentration of subsurface hydroxyl species. The reaction of methanol with  $\text{Ag}_2\text{O}$  at high temperatures was interesting in that an inhibition in silver grain growth was noted. Substantial structural modification of the silver(I) oxide material was induced by catalytic etching in a methanol/air mixture. In particular, “pin-hole” formation was observed to occur at temperatures in excess of 773 K, and it was also recorded that these “pin-holes” coalesced to form large-scale defects under typical industrial reaction conditions. Raman spectroscopy revealed that the working surface consisted mainly of subsurface oxygen and surface  $\text{Ag}-\text{O}$  species. The relative lack of subsurface hydroxyl species suggested that it was the desorption of such moieties which was the cause of the “pin-hole” formation.

**Keywords:** methanol oxidation, silver(I) oxide catalyst, nature of adsorbed species, surface structure

## 1. Introduction

Silver catalysts are widely used to convert methanol to formaldehyde at a temperature between 920 and 970 K, and at atmospheric pressure. Despite the fact that these catalysts exhibit high selectivity to formaldehyde and over 90% methanol conversion there is still a desire to further increase their performance. Additionally, several problems surround the initial catalyst activation period in a modern industrial plant. In particular, the catalyst bed may not “light-off” for many hours (even days in the worst instance) and the initial level of formic acid by-product formation can be unacceptably high. Intensive research has been dedicated to resolving the reaction mechanism [1,2] and characterizing the active site [3,4]. Nevertheless confusion still exists, due primarily to the critical influence of catalyst morphology upon the ability of silver to adsorb oxygen [5,6]. Ertl and co-workers [7,8] have shown that the silver surface undergoes large-scale reconstruction at temperatures  $> 800$  K in an oxygen atmosphere. Subsurface oxygen and a new strongly bound surface oxygen species are formed as evidenced by Raman bands at ca.  $630$  and  $800\text{ cm}^{-1}$ , respectively [8,9]. Pettinger et al. [10] recently suggested that thermal decomposition of  $\text{Ag}_2\text{O}_8\text{NO}_3$  produced a similar reconstructed silver surface. This latter result is inter-

esting in relation to the known practice of covering a silver catalyst bed with silver oxide to aid reaction “light-off”. However, almost no information has been reported to explain why this methodology should be beneficial. Our research group has employed environmental scanning electron microscopy (ESEM) to monitor structural changes in polycrystalline silver under in situ methanol oxidation conditions [11]. Pin-hole formation was observed as a consequence of recombination of subsurface hydroxyl species (produced by water and/or methanol interaction). Furthermore, extensive surface reconstruction was imaged at temperatures exceeding the Tammann value. Raman microscopy also detected the presence of substantial concentrations of oxygen associated with reconstructed silver phases following methanol oxidation.

Consequently, to elucidate the effect of doping a silver catalyst this paper reports a combined ESEM and Raman spectroscopy investigation of the reaction of  $\text{O}_2$ ,  $\text{H}_2\text{O}$ ,  $\text{CH}_3\text{OH}$  and  $\text{CH}_3\text{OH}/\text{O}_2$  with silver(I) oxide powder.

## 2. Experimental

An Electroscan ESEM model 20A instrument operating at an accelerating voltage of 30 kV was used, and images collected continuously by a videocamera.

\* To whom correspondence should be addressed.

Individual snapshots of the reaction were acquired by a videoprinter. Typically, 100 mg of silver(I) oxide (Aldrich, 99%) was placed on the heating stage in the ESEM analytical chamber. A flow of either oxygen (BOC, 99.99%, 200 ml min<sup>-1</sup>), water vapour, or methanol (BDH, AnalaR grade) vapour or methanol in air (obtained by use of a conventional saturator assembly, CH<sub>3</sub>OH/O ratio 1.2 : 1) was then passed over the sample. Catalyst heating was achieved by a programmable temperature controller which produced a heating rate of 20 K/min. More detailed post-reaction images were obtained by Jeol 890 field emission scanning electron microscope (FESEM).

Raman microscopy spectra were recorded using a Renishaw Raman microprobe spectrometer equipped with a helium–neon laser giving an incident power of ca. 1 mW and a CCD detector. Spectra were averaged over four scans and a spectral resolution of 4 cm<sup>-1</sup> employed. Spectral manipulation was performed using GramsResearch software (Galactic Industries).

### 3. Results and discussion

#### 3.1. Interaction of oxygen with Ag<sub>2</sub>O

Fig. 1 shows a series of ESEM images recorded in situ, where a sample of silver(I) oxide was exposed to a flow of oxygen and then heated to 973 K. Fig. 1a shows the characteristic structure of Ag<sub>2</sub>O powder which comprises of agglomerates or irregularly shaped particles with sizes in the range 2–5 μm. As the temperature of the oxide was raised to 578 K the grains appeared to contract (fig. 1b) and this behaviour correlated with the known decomposition temperature of silver(I) oxide to silver metal [12]. Further elevation of the catalyst temperature to 783 K (fig. 1c) was sufficient to initiate the coalescence of the small silver particles into more extended structures. This observation is in accordance with the fact that the silver catalyst is now at a temperature above the Tammann value (643 K, calculated as 0.52  $T_m$ , where  $T_m$  = melting point of silver). Since the Tammann temperature gives an indication of when lattice atoms become mobile, it is not unreasonable for the silver sample to begin to sinter. Continued heating (figs. 1e, 1f) resulted in more pronounced amalgamation of the silver moieties into large globular masses of several tens of microns in dimension (again suggesting that the silver surface was extremely mobile under the high temperature conditions).

In order to gain an insight into the surface chemistry involved, Raman microscopy was employed to identify the chemical state of the catalyst. Fig. 2a displays the Raman spectrum of the parent silver(I) oxide. Two bands were recorded at 389 and 491 cm<sup>-1</sup> and it was noted that the relative intensity of these bands was sensitive to the power of the laser used (cf. figs. 2a and 2b).

This data is entirely consistent with the reported susceptibility of Ag<sub>2</sub>O to oxidise to AgO in the presence of laser illumination [13]. The Raman spectrum of AgO contains a band at ca. 530 cm<sup>-1</sup> [14] whereas AgO is characterized by a peak at ca. 430 cm<sup>-1</sup> [13]. In contrast, following the ESEM reaction of silver(I) oxide with oxygen bands at 228, 466, 532, 582, 601, 633, 675, 755 and 966 cm<sup>-1</sup> were observed (fig. 2c). Inspection of the literature rapidly revealed that all the detected bands could not simply be assigned to oxygen species [9]. The peak at 228 cm<sup>-1</sup> was typical for weakly adsorbed molecular and/or atomically adsorbed oxygen and the band at 966 cm<sup>-1</sup> was characteristic for strongly bound molecular oxygen, probably located on a reconstructed silver surface [9]. Bao et al. [16] reported Raman bands at 632 and 802 cm<sup>-1</sup> due to oxygen species associated with a silver surface which had undergone reconstruction in an oxygen atmosphere at 780 K. The 633 cm<sup>-1</sup> peak seen in the current study is in good agreement with the observations of Bao et al. [16] and suggests that the decomposition of Ag<sub>2</sub>O in oxygen produced a reconstructed silver structure. Significantly, the band at 755 cm<sup>-1</sup> (fig. 2c) is of lower wavenumber than the value of 802 cm<sup>-1</sup> provided by Bao et al. [16]. This behaviour has been noted to occur upon reaction of a silver catalyst in water vapour under high-temperature conditions [11], and has been ascribed to the presence of subsurface OH species modifying the bonding properties of silver. The features at 466 and 582 cm<sup>-1</sup> support this latter conclusion since they are indicative of subsurface hydroxyl species located at defect sites and more extended surface planes, respectively [11,17]. Surface hydroxyl species have also been identified by Raman spectroscopy [17] on oxidised silver following contact with water. A peak at 554 ( $\nu(\text{Ag-OH})$ ) cm<sup>-1</sup> was seen which correlates with the band at 532 cm<sup>-1</sup> in fig. 2c. The remaining features at ca. 601 and 675 cm<sup>-1</sup> can be assigned to  $\nu(\text{Ag-O})$  modes of subsurface oxygen species whose bonding has been modified by the presence of subsurface hydroxyl groups in the same manner as described previously [11]. In summary, it is apparent that the oxidised silver produced in the ESEM experiment had reacted with water and carbon dioxide once exposed to air. This is not a trivial result since polycrystalline silver manufactured by electrochemical refining, which contained oxygen species indicating a reconstructed silver surface did not react with either H<sub>2</sub>O or CO<sub>2</sub> at ambient temperature (fig. 2d). Indeed, the spectrum obtained closely resembled that recorded by Bao et al. [16] for a reconstructed silver single crystal under in situ conditions. Clearly, the reactivity of the silver surface formed by decomposition of Ag<sub>2</sub>O was substantially greater than typical polycrystalline silver catalysts derived by electrochemical means. This observation is in accordance with the studies of Czanderna [18] and Seyedmonir et al. [19] which also indicated a higher rate of oxidation on silver powders and on small supported particles, relative to larger poly-

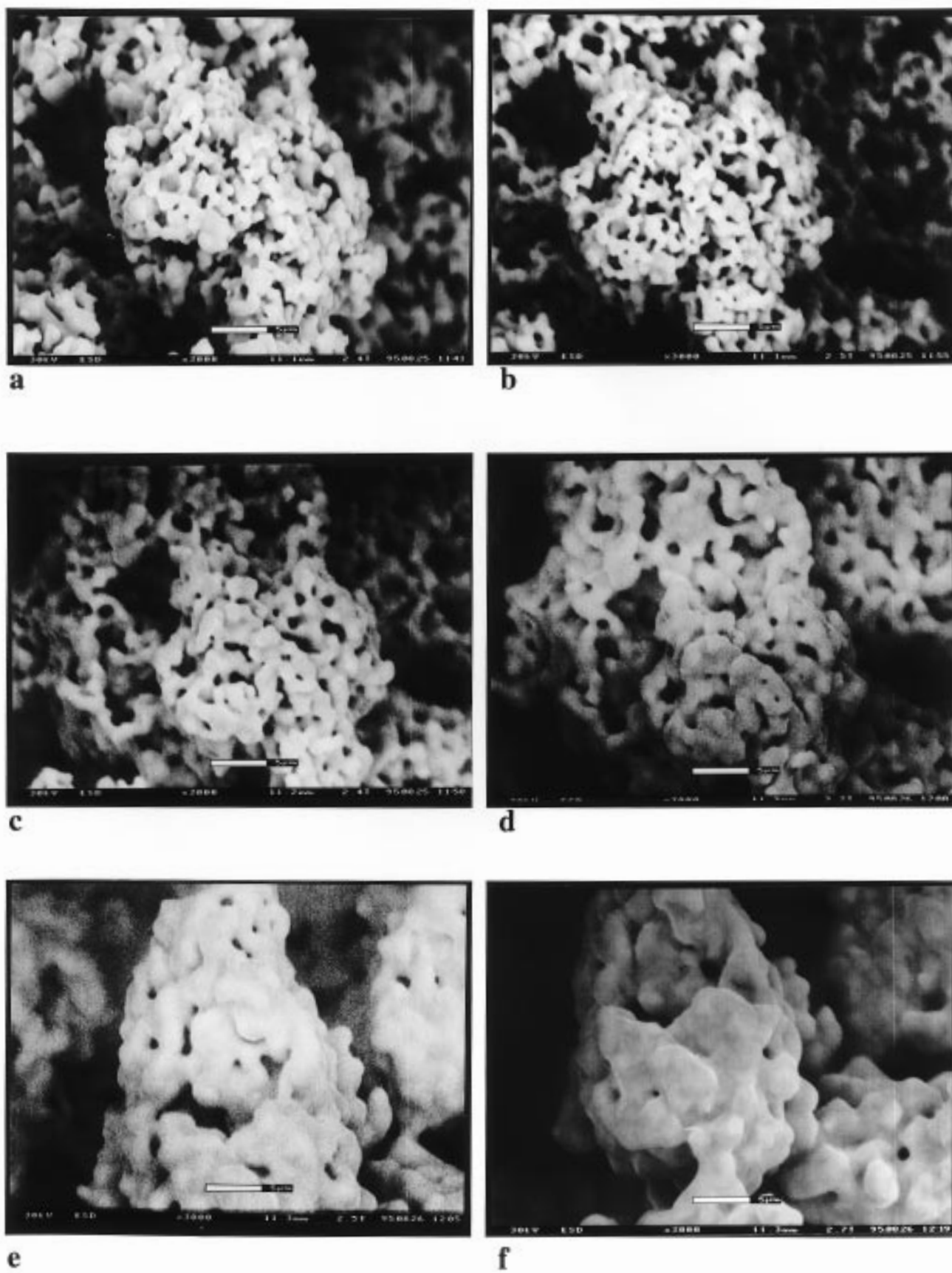


Fig. 1. ESEM images recorded during heating of  $\text{Ag}_2\text{O}$  in oxygen to a temperature of (a) 295, (b) 638, (c) 783, (d) 838, (e) 923 and (f) 973 K.

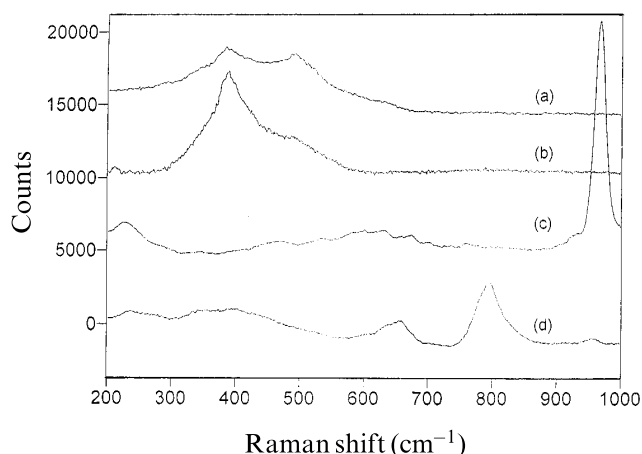


Fig. 2. Raman spectra of (a)  $\text{Ag}_2\text{O}$  (low laser power), (b)  $\text{Ag}_2\text{O}$  (high laser power), (c)  $\text{Ag}_2\text{O}$  after heating in oxygen and (d) electrochemically produced polycrystalline silver.

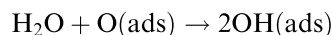
crystalline samples. This behaviour appears to be a function of the crystal faces exposed on silver [20] and also of the concentration of intergrain boundaries [21]. Albers et al. [20] demonstrated that oxygen did not adsorb on defect free  $\text{Ag}(111)$  whereas on an  $\text{Ag}(110)$  surface significant oxygen uptake is observed [22]. Recently, Tsybulya et al. [21] concluded that silver particles containing micrograin boundaries in their structure exhibited higher reactivity towards ethylene epoxidation.

### 3.2. Interaction of $\text{H}_2\text{O}$ with $\text{Ag}_2\text{O}$

Water is added to the feedstream of an industrial methanol oxidation plant to control the temperature of the catalyst bed. In addition, it has also been discovered that water can act as a promoter for the selective formation of formaldehyde [15]. Therefore, it is of interest to examine the interaction of water with  $\text{Ag}_2\text{O}$ . An ESEM experiment was performed which was completely analogous to the method described for the reaction of  $\text{Ag}_2\text{O}$  with  $\text{O}_2$  except for the fact that an atmosphere of water vapour was employed instead of oxygen. Images recorded before and after reaction are illustrated in fig. 3. In general, it can be concluded that the behaviour of silver(I) oxide heated in oxygen was comparable to the situation when water vapour was present (cf. figs. 1 and 3). Heat treatment caused the  $\text{Ag}_2\text{O}$  to decompose to produce small silver metal particles which then gradually coalesced to form comparatively large and complex structures. However, the Raman spectrum of the sample exposed to  $\text{H}_2\text{O}$  vapour did reveal that important chemical changes had occurred (fig. 4a) since bands were identified at ca. 524, ca. 572 and 644  $\text{cm}^{-1}$ . The peak at 644  $\text{cm}^{-1}$  has been reported by Pettinger et al. [23] and Millar et al. [9], who ascribed this feature to the  $\nu(\text{Ag}-\text{O})$  mode of a subsurface oxygen species associated with a reconstructed silver surface. Recently, Bao et al. [17] noted that the interaction of water or hydrogen with sub-

surface oxygen species resulted in the creation of subsurface hydroxyl groups ( $\nu(\text{Ag}-\text{OH})$ , 575  $\text{cm}^{-1}$ ). The excellent correlation of this band with the peak at ca. 572  $\text{cm}^{-1}$  in the current study supports a similar assignment. Finally, the remaining feature at ca. 524  $\text{cm}^{-1}$  is ascribed to the  $\nu(\text{Ag}-\text{OH})$  vibration of a surface hydroxyl species, a view supported by Bao et al. [17] since they observed a band at 554  $\text{cm}^{-1}$  as a consequence of water/ $\text{O}_2$  interaction with an  $\text{Ag}(111)$  crystal at 300 K. Another less probable appointment is that the 524  $\text{cm}^{-1}$  band may be indicative of a silver oxide species. This assignment is discredited due to the fact that silver(I) oxide decomposition was definitely observed in the ESEM images. Furthermore, more extensively dissolved oxygen atoms in the bulk silver lattice (which are feasible under the applied conditions) are represented by a peak at 485  $\text{cm}^{-1}$  [9].

The role of water in the methanol oxidation process is a subject of some debate. It has been postulated that water can act as a reducing agent for surface oxygen species (which are suspected of being the cause for non-selective oxidation of formaldehyde [24]) according to the reaction



Similarly, Kurina and Morosov [25] proposed that water adsorbed at the sites where formaldehyde combustion occurred, thus inhibiting this side-reaction. Alternatively, Bao et al. [17] have also inferred that the recombination of hydroxyls creates a strongly bound oxygen species which is active for methanol oxidation. To investigate the influence of water in greater detail an experiment was conducted where silver(I) oxide was initially heated in oxygen to 973 K and then exposed to water vapour at ca. 623 K. A typical Raman spectrum (fig. 4b) consists of an intense band at 570  $\text{cm}^{-1}$  attributed to the  $\nu(\text{Ag}-\text{O})$  mode of subsurface hydroxyl species [17]. This effect was not observed at any location on the silver(I) oxide sample which had been heated in  $\text{H}_2\text{O}$  vapour. Careful examination of the catalyst surface resulted in the attainment of Raman spectra of the type shown in fig. 4c which allowed clearer identification of the species present. Bands were evident at ca. 470, ca. 520, 605 and 680  $\text{cm}^{-1}$ . The peaks at 680 and 605  $\text{cm}^{-1}$  are proposed to be due to vibrations of  $\text{Ag}=\text{O}$  and  $\text{O}$  (sub)species associated with a reconstructed silver surface, whose frequencies have been modified by the presence of hydroxyl groups incorporated in the near-surface region of silver [9,11]. In accordance with Bao et al. [17], the band at 520  $\text{cm}^{-1}$  is ascribed to the  $\nu(\text{Ag}-\text{OH})$  mode of surface hydroxyl groups. Finally, the peak at 470  $\text{cm}^{-1}$  suggests the presence of more extensively dissolved atomic oxygen in the silver lattice [9]. It is therefore postulated that the reconstructed silver surface had reacted with water vapour to differing degrees and a summary of the band positions for each adsorbate is given in table 1.

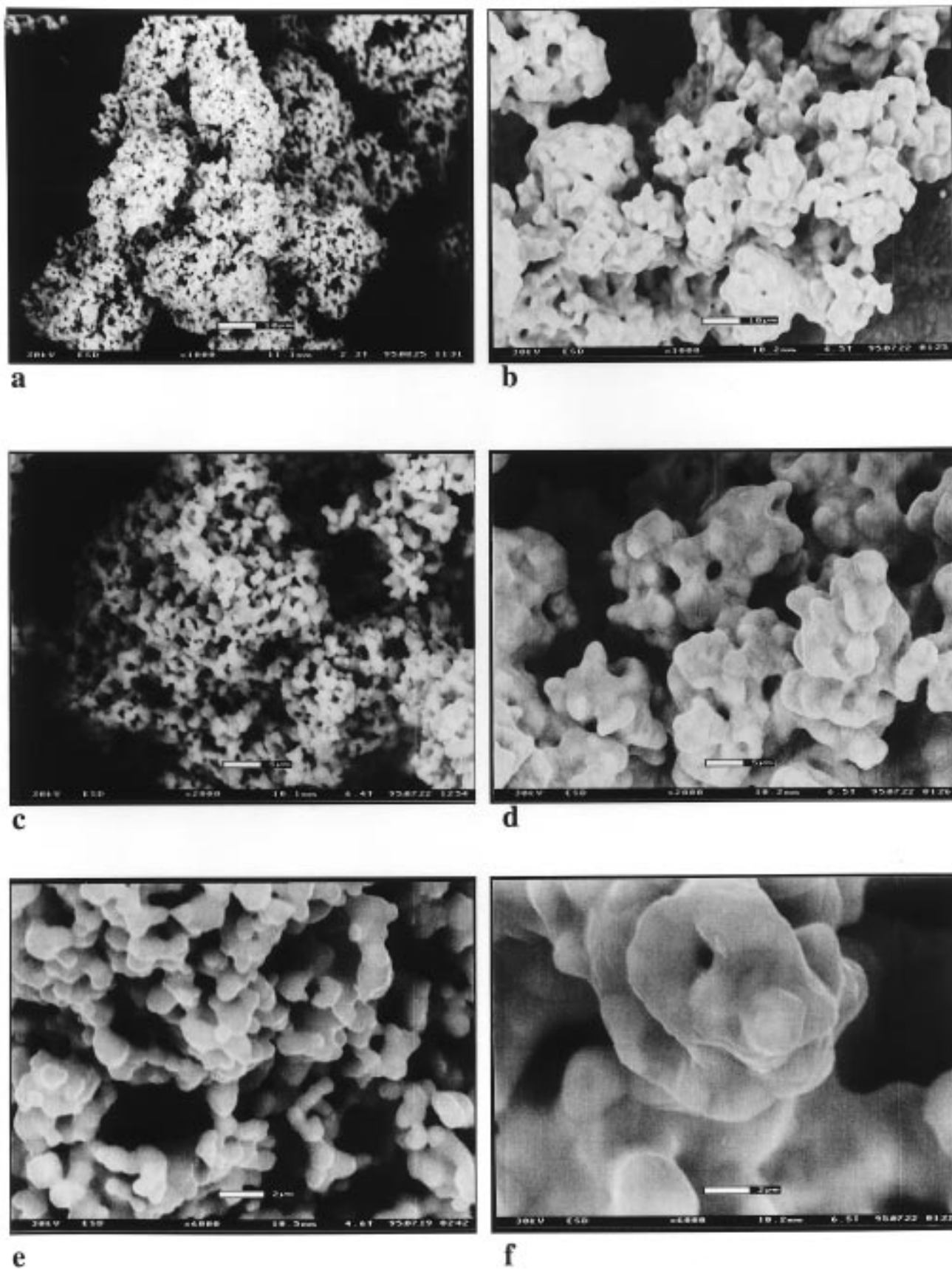


Fig. 3. ESEM images of  $\text{Ag}_2\text{O}$  before (a), (c), (e) and after reaction with water vapour at 973 K (b), (d) and (f).

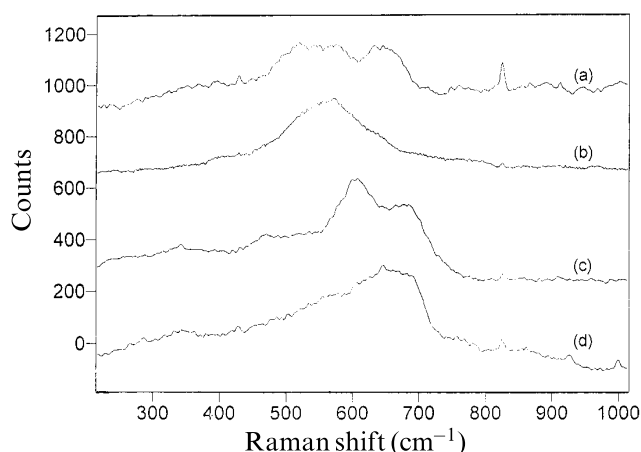


Fig. 4. Raman spectra of  $\text{Ag}_2\text{O}$  after heat treatment with (a) water vapour, (b) and (c) oxygen then water vapour, and (d) oxygen/methanol.

### 3.3. Interaction of methanol with silver(I) oxide

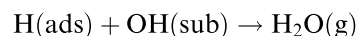
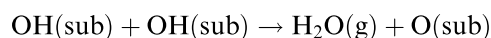
An ESEM investigation of the interaction of methanol vapour with  $\text{Ag}_2\text{O}$  was performed, and images recorded pre- and post-reaction. The only notable feature was that a significant inhibition in grain growth was observed under the applied conditions (relative to the case with either  $\text{O}_2$  or  $\text{H}_2\text{O}$ ). Raman spectra of the so-formed silver sample did not contain any notable features. This latter result is of relevance with regards to the inhibition of grain growth, in that it is known [26] that the surface mobility of silver atoms is critically influenced by adsorbate interaction. In particular, oxygen present in subsurface locations causes pronounced surface restructuring [7]. It was only with  $\text{O}_2$ ,  $\text{H}_2\text{O}$  or  $\text{O}_2/\text{CH}_3\text{OH}$  that subsurface oxygen species were determined in this study, in contrast no such species were formed when methanol

was utilized. Consequently, the extent of silver sintering was substantially reduced.

### 3.4. Interaction of methanol/oxygen with silver(I) oxide

Silver(I) oxide was exposed to a flow of oxygen saturated with methanol and imaged in situ by ESEM while the temperature was raised to 973 K. Fig. 5 shows that substantial morphological changes were induced in the catalyst by the presence of methanol. Elevation of the sample temperature to 773 K (fig. 5b) resulted in the appearance of a small concentration of “pin-holes” of ca.  $0.2\text{--}0.5\ \mu\text{m}$  in dimension. Further heating (figs. 5c, 5d) not only caused significant enhancement in the rate of “pin-hole” formation but also the holes themselves gradually increased in size to ca.  $0.5\text{--}1.0\ \mu\text{m}$ . Interestingly, as industrial reaction temperatures were achieved (figs. 5e, 5f) it was apparent that the “pin-holes” were coalescing to form large defects in the order of several microns in length. The corresponding Raman spectrum (fig. 4d) revealed a complex profile between  $400$  and  $700\ \text{cm}^{-1}$ . Deconvolution of this feature suggested the presence of subbands at ca.  $500$ ,  $578$ ,  $611$ ,  $646$ ,  $689$  and  $753\ \text{cm}^{-1}$ . As before, the subbands at  $500$  and  $578\ \text{cm}^{-1}$  can be assigned to surface and subsurface hydroxyl species, respectively. The peak at  $640\ \text{cm}^{-1}$  is characteristic of subsurface oxygen [9,18] whereas the band at  $611\ \text{cm}^{-1}$  is probably associated with a subsurface oxygen neighboring a subsurface hydroxyl species. Finally, the peaks at  $689$  and  $753\ \text{cm}^{-1}$  are ascribed to  $\nu(\text{Ag}=\text{O})$  modes of strongly bound atomic oxygen atoms situated on a silver surface containing high and moderate amounts of subsurface hydroxyl species, respectively. Significantly, subsurface OH groups were never found to be the dominant species in the Raman spectra for this sample.

Pin-hole formation in silver catalyst has been reported by several authors [26,27] and is proposed to occur via the following reactions:



Bao et al. [26] have indicated that the “driving force” for hole production is the generation of hydrostatic pressure in subsurface locations. Recently, Millar et al. [9] obtained confirmation for this hypothesis using ESEM to image hole formation on polycrystalline silver catalyst. Clear evidence for subsurface explosions was provided as considerable debris was found in the vicinity of the “pin-holes”.

Fig. 6 illustrates the structural differences between the catalyst which was reacted with water and the one which was exposed to methanol/ $\text{O}_2$ . In accordance with the theory that subsurface explosions had occurred when methanol was present, significant quantities of debris were observed in figs. 6b, 6d and 6f. Common to

Table 1  
Band positions of adsorbates

| Band position                                 | Species   |
|---|---|
| $228\ \text{cm}^{-1}$                         | weakly adsorbed molecular oxygen and/or atomic oxygen                               |
| $389\ \text{cm}^{-1}$ , $430\ \text{cm}^{-1}$ | bulk $\text{Ag}_2\text{O}$  |
| $466\ \text{cm}^{-1}$                         | subsurface hydroxyl (defect sites)  |
| $470\text{--}485\ \text{cm}^{-1}$             | dissolved atomic oxygen   |
| $491\ \text{cm}^{-1}$ , $530\ \text{cm}^{-1}$ | bulk $\text{Ag}_2\text{O}$  |
| $500\text{--}532\ \text{cm}^{-1}$             | surface hydroxyl  |
| $570\text{--}582\ \text{cm}^{-1}$             | subsurface hydroxyl (extended surface planes)                                       |
| $601\text{--}611\ \text{cm}^{-1}$             | subsurface oxygen<br>(neighbouring subsurface hydroxyl)                             |
| $633\text{--}644\ \text{cm}^{-1}$             | subsurface oxygen<br>(reconstructed silver surface)                                 |
| $675\text{--}689\ \text{cm}^{-1}$             | $\text{Ag}=\text{O}$ on reconstructed surface<br>(neighbouring subsurface hydroxyl) |
| $750\text{--}755\ \text{cm}^{-1}$             | $\text{Ag}=\text{O}$ on reconstructed surface<br>(subsurface hydroxyl)              |
| $966\ \text{cm}^{-1}$                         | strongly adsorbed molecular oxygen<br>(at reconstructed surface)                    |



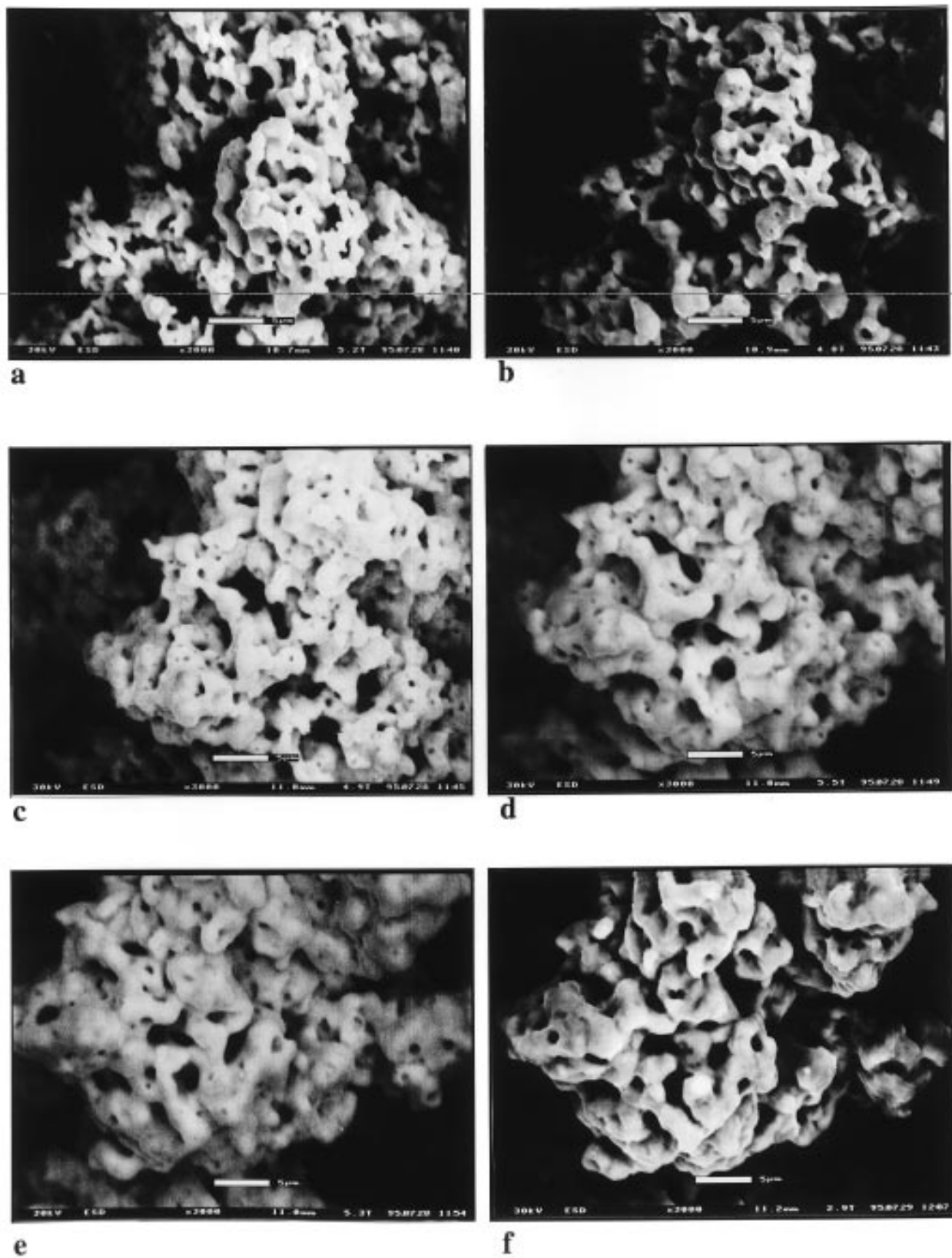


Fig. 5. ESEM images recorded during heating of  $\text{Ag}_2\text{O}$  in an oxygen/methanol mixture to a temperature of (a) 623, (b) 773, (c) 823, (d) 883, (e) 943 and (f) 973 K.

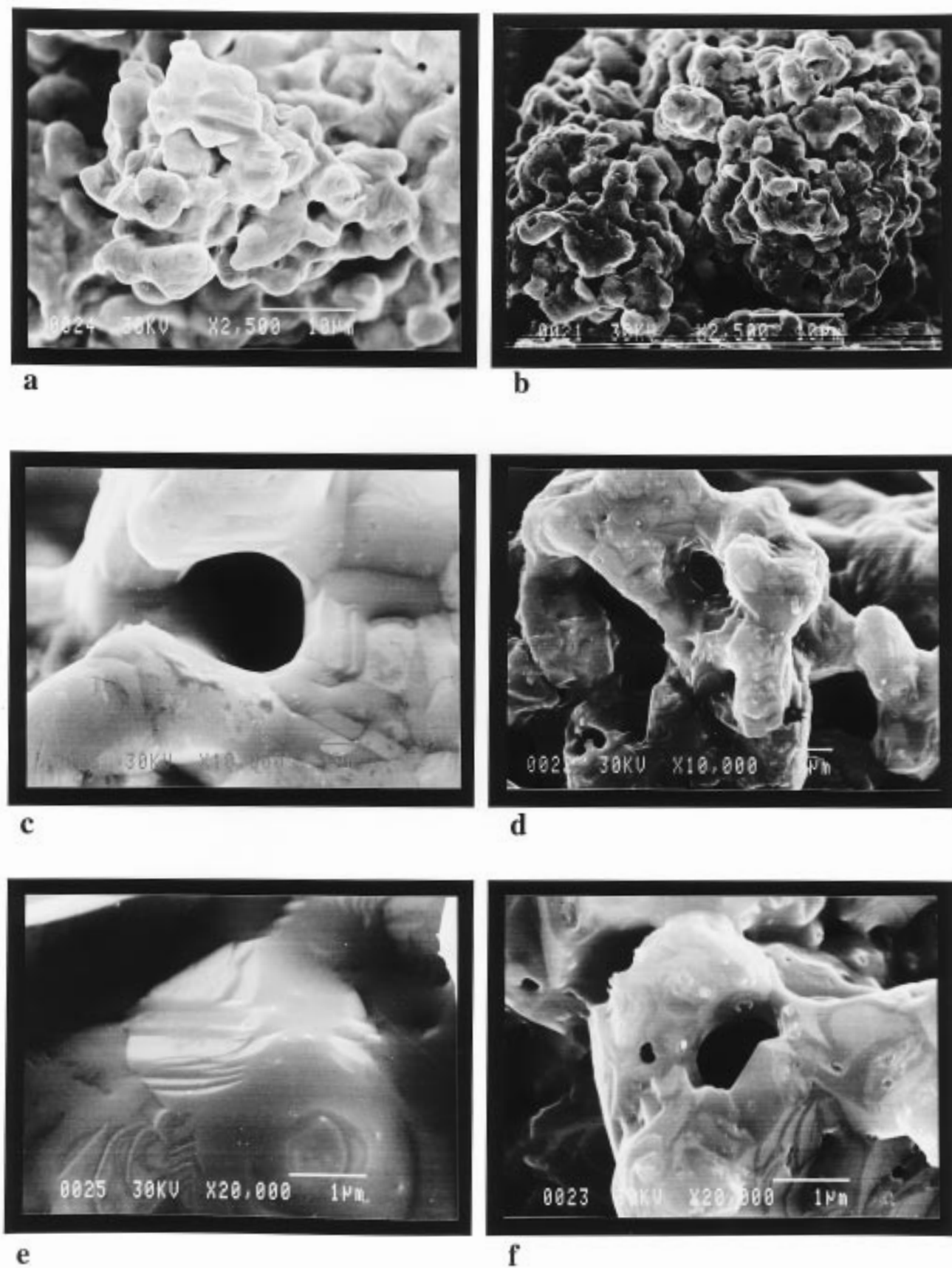


Fig. 6. FESEM images of the silver structure following reaction of AgO with water vapour (a), (c), (e) and oxygen/methanol (b), (d), (f).



both systems were the presence of extensive “terrace and step” structures on the catalyst surface (figs. 6e, 6f). Ertl and co-workers [7] employed REM and SEM to demonstrate that the interaction of oxygen with silver foil at high temperature caused pronounced surface restructuring to produce a “terrace and step” structure similar to that recorded in this study. Furthermore, it was concluded from RHEED and STM data that this reconstruction resulted in the incorporation of subsurface oxygen species in the layer directly below the silver surface. The Raman spectra outlined in fig. 4 are in excellent agreement with the electron microscopy data, that  $\text{Ag}_2\text{O}$  decomposition in the presence of either  $\text{H}_2\text{O}$  or  $\text{CH}_3\text{OH}/\text{O}_2$  resulted in a reconstructed silver surface.

#### 4. Conclusions

Polycrystalline silver derived from  $\text{Ag}_2\text{O}$  decomposition was found to be exceptionally reactive due to a combination of the nature of the crystal faces exposed and the number of intergrain boundaries. Moreover, incorporation of oxygen and/or hydroxyl species into the subsurface region of silver was determined to facilitate surface restructuring.

#### References

- [1] I.E. Wachs and R.J. Madix, *Surf. Sci.* 76 (1978) 531.
- [2] L. Lefferts, J.G. van Ommen and J.R.H. Ross, *Appl. Catal.* 23 (1986) 385.
- [3] G.J. Millar, J.B. Metson, G.A. Bowmaker and R.P. Cooney, *J. Chem. Soc. Chem. Commun.* (1994) 1717.
- [4] A.N. Pstryakov and A.A. Davydov, *Appl. Catal. A* 120 (1994) 7.
- [5] G.R. Meima, R.J. Vis, M.G.J. van Leur, A.J. van Dillen, J.W. Geus and F.R. van Buren, *J. Chem. Soc. Faraday Trans. I* 85 (1989) 279.
- [6] J.K. Plischke and M.A. Vannice, *Appl. Catal.* 42 (1988) 255.
- [7] X. Bao, J.V. Barth, G. Lehmppfuhl, R. Schuster, Y. Uchida, R. Schlögl and G. Ertl, *Surf. Sci.* 284 (1993) 14.
- [8] X. Bao, M. Muhler, B. Pettinger, R. Schögl and G. Ertl, *Catal. Lett.* 22 (1993) 215.
- [9] G.J. Millar, J.B. Metson, G.A. Bowmaker and R.P. Cooney, *J. Chem. Soc. Faraday Trans.* 91 (1995) 4149.
- [10] B. Pettinger, X. Bao, I. Wilcock, M. Muhler, R. Schögl and G. Ertl, *Angew. Chem. Int. Ed. Engl.* 33 (1994) 85.
- [11] G.J. Millar, M.L. Nelson and P.J.R. Uwins, submitted.
- [12] I. Náray-Szabó and K. Popp, *Z. Anorg. Allg. Chem.* 322 (1963) 286.
- [13] R. Kotz and E.J. Yeager, *J. Electroanal. Chem.* 111 (1980) 105.
- [14] J.A. Allen and P. Scaife, *Austr. J. Chem.* 19 (1966) 715.
- [15] H. Sperber, *Chemie-Ing. Techn.* 41 (1969) 962.
- [16] X. Bao, B. Pettinger, G. Ertl and R. Schögl, *Ber. Bunsenges. Phys. Chem.* 97 (1993) 322.
- [17] X. Bao, M. Muhler, B. Pettinger, Y. Uchida, G. Lehmppfuhl, R. Schlögl and G. Ertl, *Catal. Lett.* 32 (1995) 171.
- [18] A.W. Czanderna, *J. Phys. Chem.* 68 (1964) 2765.
- [19] S.R. Seyedmonir, D.E. Strohmayer, G.L. Geoffroy, M.A. Vannice, H.W. Young and J.W. Linowski, *J. Catal.* 87 (1984) 424.
- [20] H. Albers, J.M.M. Droog and G.A. Bootsma, *Surf. Sci.* 64 (1977) 1.
- [21] S.V. Tsybulya, G.N. Kryukova, S.N. Goncharova, A.N. Shmakov and B.S. Bal'zhinimaev, *J. Catal.* 154 (1995) 194.
- [22] H.A. Engelhardt and D. Menzel, *Surf. Sci.* 57 (1976) 591.
- [23] B. Pettinger, X. Bao, I.C. Wilcock, M. Muhler and G. Ertl, *Phys. Rev. Lett.* 72 (1994) 1561.
- [24] L. Lefferts, J.G. van Ommen and J.R.H. Ross, *Appl. Catal.* 31 (1987) 291.
- [25] L.N. Kurina and V.P. Morosov, *Russ. J. Phys. Chem.* 50 (1976) 538.
- [26] X. Bao, G. Lehmppfuhl, G. Weinberg, R. Schögl and G. Ertl, *J. Chem. Soc. Faraday Trans.* 88 (1992) 865.
- [27] L. Lefferts, J.G. van Ommen and J.R.H. Ross, *Appl. Catal.* 34 (1987) 329.